AoA Estimation from Array of Single-board Devices with Single-antenna Wi-Fi chip

SHIYUAN ZHUANG[1] HAN LIN[1] KOTA TSUBOUCHI[2] NOBUHIKO NISHIO[3]
MASAMICHI SHIMOSAKA[1]

Abstract: Angle of Arrival (AoA) estimation has received considerable attention as a key solution in indoor positioning systems, particularly using Channel State Information (CSI) derived from Wi-Fi packets. Traditional approaches often leverage multi-antenna MIMO devices to perform MIMO-based time-of-arrival analyses across different antennas. However, these devices have been discontinued and are increasingly difficult to acquire, while single-board CSI scanners pose challenges for accurate AoA prediction. In this work, we propose a novel deployment strategy that arranges multiple single-board, single-antenna devices in an array to capture CSI from the same packet. We combine these measurements via matching MAC addresses and sequence numbers, then apply a learning-based AoA estimation model to obtain angle estimates. Our approach offers a more flexible and easily deployable solution with readily available hardware, serving as an effective sensor platform for downstream applications using AoA.

Keywords: Wi-Fi CSI, Angle of Arrival, Single-board Sensor

1. Introduction

In recent years, Angle of Arrival (AoA) estimation of wireless signal has received considerable attention as a key solution in indoor positioning systems and human activity recognition. Among them, WiFi-based AoA estimation is notable for their ability to use existing protocols without additional equipment, reducing deployment costs [1].

For WiFi-based approach, Channel State Information (CSI) has been extensively studied for AoA estimation in recent years. It has the ability to provide complex features by capturing frequency attenuation information, compared with traditional Receive Signal Strength Indicator (RSSI) based approach [2] [3].

Unlike RSSI, CSI collection requires specialized equipment. Most of the recent commercial devices lack the ability of extracting CSI from Wi-Fi signal. Traditional approaches of getting AoA estimation from CSI often leverage multi-antenna devices to perform Multi Input Multi Output (MIMO) based time-of-arrival analyses across different antennas.

However, these MIMO devices have been discontinued and are increasingly difficult to acquire in the market. Meanwhile, the use of Single Input Single Output (SISO) devices raises concerns about AoA estimation performance, as they fail to provide sufficient features.

To address these issues, this paper presents a method that utilizes an array of multiple SISO devices to extract CSI information for AoA estimation. This work provides an effective foundational solution for subsequent AoA-driven downstream applications, such as indoor localization and human activity recognition.

The contributions of this work include the followings:

- We propose a novel approach that utilizes an array of inexpensive and commercially available single-board SISO computers to collectively capture CSI data.
- We design an MLP-based learning model for AoA estimation, using the combined CSI amplitudes as input.
- We offer an effective foundational solution for subsequent AoA-driven applications using easily obtainable commercial SISO devices.

2. Related work

2.1 Channel State Information for Wi-Fi sensing

In recent years, CSI has gained widespread application in the fields of Wi-Fi sensing and localization. CSI is a physical layer metric used to reflect frequency-selective fading. It is extracted from pilot signals by certain specialized devices and provides detailed information on the phase and amplitude attenuation of individual subcarriers. The amplitude and phase of the CSI are influenced by the movements and displacements of the transmitter, receiver, and nearby objects and people.

CSI captures more complex reflection information than the traditional RSSI. It reflects the attenuation at multiple subcarrier frequencies, when traditional RSSI only represents the overall signal attenuation. Therefore, CSI has become a preferred choice in many studies, where it has replaced RSSI in various applications. For example, Human Activity Recognition benefits from the complex reflection information provided by CSI. For instance, features of CSI can be learned through deep neural networks to recognize certain activities [4] [5]. Also, fingerprint-based local-

[1] Department of Computer Science, School of Engineering, Institite of Science Tokyo
[2] LY Corporation
[3] Ritsumeikan University

ization with CSI is getting popular [6].

However, CSI is heavily influenced by physical reflections. Many studies focus on analyzing CSI to extract useful physical information, such as AoA [7] and Time of Flight (ToF), concluded in [8]. These metrics help in deriving meaningful features from CSI.

2.2 Angle of Arrival estimation by CSI

Angle of Arrival (AoA) from CSI can reflect the angle at which a signal arrives, making it applicable in many fields such as signal source localization [9] and human activity recognition [10]. CSI can be used for AoA estimation of wireless signal, because CSI reflect detailed channel states through signal attenuation and phase variations. Some methods use CSI phase differences across different antennas to extract AoA of the signal [7] [11].

Since phase is easily affected by sampling clock asynchrony, some recent studies have utilized amplitude or a combination of amplitude and phase to extract AoA information. For example, AoA-net [12] uses optimal subcarriers for estimating the AoA using a deep neural network.

However, obtaining suitable devices for AoA estimation using CSI remains a significant challenge. Most existing methods for AoA estimation rely on specialized MIMO devices [7] [11] or custom-designed WiFi access points [12] for CSI data collection, which are distinct from commercially available devices commonly used today.

2.3 Traditional CSI data collection tools for AoA estimation

To extract effective phase information, traditional devices are equipped with the same core and support MIMO capabilities. As one of the most classic CSI collection tools, the Linux 802.11n CSI Tool is widely used in research [13]. It collects CSI data from packets using the Intel 5300 NIC on Linux systems, obtaining values for 30 subcarriers per packet. Equipped with three antennas, the Intel 5300 NIC is particularly notable for its ability to extract stable phase information, making it widely used in research [14].

However, this device has long been discontinued, and compatible components are difficult to obtain, making it challenging to acquire CSI for new research. Intel 5300 NIC was released in 2008, and computers with the device should have being sold around that time and are discontinued by manufacturers as well. Therefore, downstream applications using AoA estimates from CSI requires a new tool that is more readily available, easier to deploy, scalable, and capable of obtaining relatively accurate AoA.

2.4 ML-based processing on CSI

Recently, machine learning-based approaches for processing CSI have garnered significant attention and research interest. Since CSI vectors can capture attenuation information across multiple channels, machine learning methods are advantageous for learning hidden features. For example, DeepAoA+ [15] uses a domain-specific model to estimate the AoA of incoming signals from CSI phase, while AoA-net [12] uses CSI amplitude for estimating the AoA using a deep neural network.

However, mainstream methods still rely on extracting signal paths using phase differences between antennas on MIMO devices. ML-based approaches for obtaining AoA are less common, likely because such methods tend to capture the complex environmental information, making cross-domain estimation challenging to achieve.

3. Proposed Method

3.1 Array of single-board devices with single-antenna Wi-Fi chip

We employ a sensor array of multiple single-board devices with single-antenna Wi-Fi chip to extract additional features. The device is fully SISO and only one antenna is attached to the board, but with multiple of these devices in the array, it is possible to make the sensor array serve as a MIMO device.

Typically, MIMO devices are used to extract CSI information received by multiple antennas and predict the signal's AoA through signal processing or machine learning methods. These devices process data from multiple antennas using a single core, ensuring clock synchronization across antennas and avoiding synchronization errors that could affect phase measurements.

However, SISO devices only have a single input antenna, making it impossible to capture phase differences between multiple antennas. Additionally, the CSI collected by SISO devices is less detailed, limiting their accuracy in AoA estimation compared to MIMO devices.

In order to address this issue, multiple SISO devices can be arranged in an array and collect CSI data together, as shown in Fig. 1. Each device collects CSI independently from its single antenna, and the CSI from the same packet across different SISO devices is combined for estimation.

However, since each SISO device operates with its own board, the clocks across their antennas are difficult to synchronize, making phase differences unreliable. Therefore, we use only CSI amplitude for estimation.

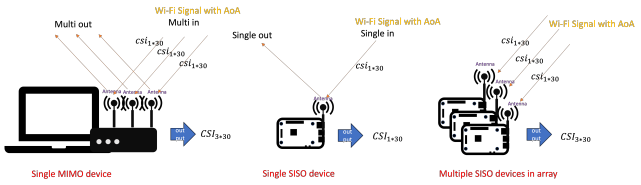

Fig. 1 Collectible CSI from MIMO device, SISO device and Array of SISO devices(Ours)

3.2 CSI data processing

3.2.1 Data packet matching

With our proposed sensor array, the packet is collected by multiple devices multiple times, so it is necessary to match the CSIs belong to the same wireless packet. We propose using MAC address, Sequence number and Time of Arrival within the packet to match the received CSI data of the same packet.

For frames such as Probe Request Frames, in which the MAC address and sequence number are randomized, we can use this information to gather the CSI of the same packet from different devices.

Fig. 2 Properties in frame information for frame matching of Probe Request Frame and Block ACK Frame

However, the method cannot be applied to some types of the frame. For the frames with Wi-Fi connection, the MAC and sequence number may not change over the time series of packets, such as Block ACK frames, as in Fig. 2. These packets are sent when using ping command in the mobile device, while sequence number field of this type of frame is always the same over time.

To address this issue, we design an algorithm that matches data packets based solely on their time-of-arrival differences within a specified threshold. Since the SISO devices are positioned very close to each other, the arrival timestamps of the same packet across the three devices have only small difference. By setting the ping transmission time interval higher than this timestamp difference, we can reliably determine whether two pieces of data originate from the same packet or from different packets. For packets from different transmissions, the timestamp difference is determined by the ping frequency, providing a clear basis for distinguishing and matching the data.

In the actual setup, the time difference between two consecutive ping packets is approximately 100[ms], while the arrival time difference of the same packet across different devices is within 25[ms].

3.2.2 CSI data normalization and combination

For data processing, we apply packet-level normalization to the CSI amplitude from each receiver and simply concatenate the vectors into the input vector of the estimator. CSI data contains phase and amplitude information, but the phase information is not reliable over the devices, which is why we extract only amplitudes of the CSI to get AoA estimates. Normalization is applied to each CSI amplitude vector because these values are affected by automatic gain control, leading to significant variations in absolute amplitude. By normalizing the vectors, we focus on their relative variations rather than their actual amplitudes, allowing the features to better capture meaningful information.

In the frequency domain, the multipath causes frequency-selective fading, which is characterized by Channel Frequency Response (CFR). A single value of CFR is defined as

$$x(f_j) = \|x(f_j)\| e^{j\angle x(f_j)} \tag{1}$$

where $x(f_j)$ is a sample at the j^{th} subcarrier, which is a complex number. This value refers to the fading scale of the signal at the receiver of a certain frequency. For a fixed channel the subcarrier index is bounded with an only frequency, so CFR uses the subcarrier index as a parameter. CSI is a collection of CFR over all the subcarriers. Thus, we can define $\boldsymbol{h}(m,k)$ as the CSI data of packet m, received by receiver k. There is:

$$\boldsymbol{h}(m,k) = [x(f_1), x(f_2), x(f_3), \ldots, x(f_J)]^{\mathsf{T}} \tag{2}$$

where J is the number of subcarriers. Here, J equals to 30. We use the absolute value to get only amplitude of each CFR.

$$|\boldsymbol{h}(m,k)| = [|x(f_1)|, |x(f_2)|, |x(f_3)|, \ldots, |x(f_J)|]^{\mathsf{T}} \tag{3}$$

Then, we conduct normalization for $\boldsymbol{h}(m,k)$. Normalization will make the data mainly reflect the changes instead of the actual strength. Thus we have $\boldsymbol{g}(m,k)$ as normalized CSI data of packet m received by receiver k. Here, $\boldsymbol{g}(m,k)$ is defined as:

$$\boldsymbol{g}(m,k) = [c(f_1), c(f_2), c(f_3), \ldots, c(f_J)]^{\mathsf{T}}, \tag{4}$$

and each element is calculated by:

$$c(f_j) = \frac{|x(f_j)| - \mu(|\boldsymbol{h}(m,k)|)}{\sigma(|\boldsymbol{h}(m,k)|)}, 1 \le j \le J, \tag{5}$$

in which $\mu(|\boldsymbol{h}(m,k)|)$ represents the mean value of $|\boldsymbol{h}(m,k)|$, while $\sigma(|\boldsymbol{h}(m,k)|)$ represents the standard deviation value of $|\boldsymbol{h}(m,k)|$.

Finally, we have the input vector for packet m, $\boldsymbol{i}(m)$ by combining all the CSI data of the packet received by all the receivers.

$$\boldsymbol{i}(m) = \begin{bmatrix} \boldsymbol{g}(m,1) \\ \boldsymbol{g}(m,2) \\ \vdots \\ \boldsymbol{g}(m,K) \end{bmatrix}, \tag{6}$$

where K is the number of receivers. Therefore, for each packet m, $\boldsymbol{g}(m,k) \in \mathbb{R}^J$, J is the number of subcarriers, and the final input vector has $\boldsymbol{i}(m) \in \mathbb{R}^{KJ}$.

3.3 Learning-based AoA estimation with CSI from multiple SISO devices

To estimate AoA using CSI amplitudes, we propose a learning-based method that utilizes a Multilayer Perceptron (MLP) with

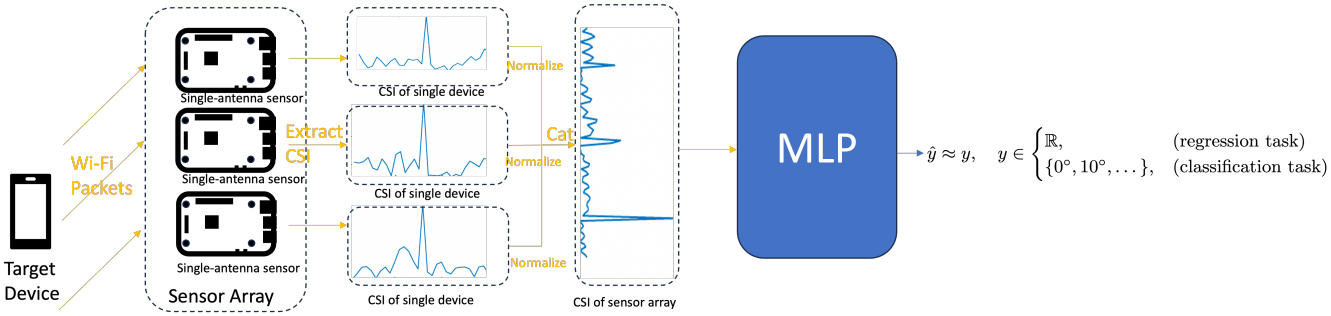

Fig. 3 MLP based AoA estimation from multiple SISO CSIs

pre-processed CSI vectors as input. By adjusting the output layers, we validate its performance through both classification and regression tasks. Specifically, we deploy a 5-layer MLP and modify the final layers to adapt to the requirements of each task. The structure is shown in Fig. 3.

Angles are continuous data, but we choose classification because it is also a traditional solution for AoA estimation and is more straightforward to implement. This method divides the angle range into equal-sized classes and assigns samples to their corresponding angle category. The width of each angle class affects the estimation results; if the width is too large, even perfectly correct classifications will still result in angle errors proportional to the class width.

For the classification task, we use a softmax layer in the final layer of the MLP to output the class probabilities and then map the class labels back to the corresponding angles. The Negative Log Likelihood (NLL) loss is applied to the classification task as a loss function.

For the regression task, we use a fully connected layer at the end to obtain a single numerical prediction result. We apply mean squared error (MSE) loss as a loss function for regression estimation.

4. Experiment Results

In this section, we designed experiments to evaluate the performance of our AoA prediction system under different settings, including the use of classification or regression models, varying the number of devices, different distances between the transmitter and the receiver, as well as varying spacing between the devices themselves.

4.1 Evaluation Protocol

4.1.1 Implementation

In the experiments, we used up to three Raspberry Pi 4B devices as representatives of the single-board devices described earlier, as shown in Fig. 4. They were all equipped with the Nexmon [16] tool to extract CSI from the frames.

To align the single-board devices into an array, we used a 3D printer to produce a framework for Raspberry Pi 4B, and each framework had 4 sharpened legs to attach solidly to a foam block. This setup allowed us to easily adjust the number of devices as well as the spacing between each device.

We used two devices as transmitters: the Google Nexus 5 and the iPhone 14 Pro. The former was used in earlier experiments to transmit probe request frames. The transmission frequency of the Nexus 5 was extremely low, approximately one packet every few seconds to ten seconds. Due to its low frequency, we adopted the iPhone 14 Pro in the other experiments, utilizing its application and the ping command to continuously send packets at a transmission frequency of around 10Hz.

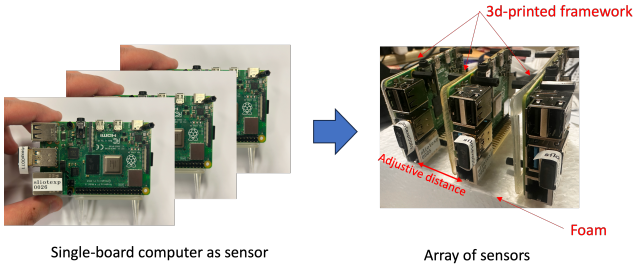

Fig. 4 Prototype of sensor array with multiple Raspberry Pi 4B

4.1.2 Data collection

We collected two datasets to comprehensively evaluate the performance of our AoA estimation system. The first dataset focused on assessing the performance of the AoA classification task, while the second dataset was designed to validate the regression task over a wider angle range with varying patterns.

For the first dataset we collected data for six classes with AoA of 0, 10, 20, 30, 40 and 45 degrees. For this dataset, we defined the positive y-axis as the 0 degree AoA, and for the 0 degree category, the distance between the transmitter and receiver was 1.5 meters. The data packets were passively transmitted as probe request frames by a Google Nexus 5 that was not connected to a network. We used a frame control field filter to ensure only these types of frames were captured. The deployment is shown in Fig. 5. Note that in this dataset, the collect data used category labels as the ground truth labels, rather than the actual numerical AoA.

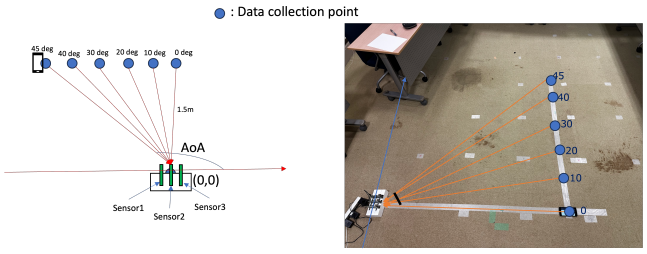

Fig. 5 Dataset 1 for AoA classification

In the second dataset, we minimized the impact of propagation distance on CSI by keeping the distance fixed and demonstrated that forming an array with multiple devices achieved better AoA prediction performance, thereby validating the effectiveness of our approach.

We set up data collection points at intervals of 15 degrees within the range of 0 degrees to 180 degrees, resulting in a total of 13 points, as in Fig. 6. An iPhone 14 Pro continuously sent data packets using the ping command at a transmission rate of 10 packets per second. At each point, 1,200 valid data frames were collected per device. Data was collected at two different distances, 1m and 2m, and using two different device spacings (the distance between single-board devices), set at 2cm and 4cm, respectively.

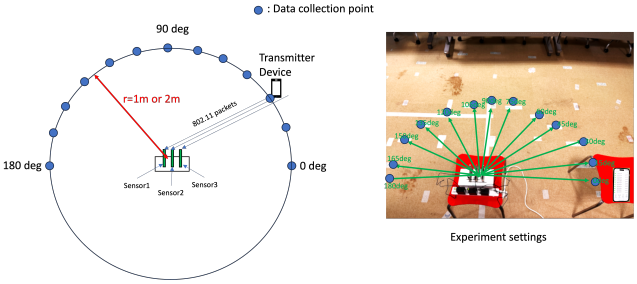

Fig. 6 Dataset 2 for regression validation with different settings of distance, number of devices and spacing

4.1.3 Evaluation Metrics

We used both classification accuracy and Mean Absolute Error (MAE) to evaluate our performance for different tasks. For the classification model, accuracy and a confusion matrix were used for analysis. For the regression model, the MAE was employed as the evaluation metric. Lower MAE refers to better performance in the AoA estimation task.

However, the classification accuracy only indicates whether a sample can be correctly assigned to an angle range. Since angles are continuous numerical values, achieving high accuracy does not necessarily imply the ability to accurately predict AoA on a continuous scale.

4.2 Results on three single-board devices

4.2.1 Classification Performance

In the first experiment, we used the first dataset which contained CSI data with 6 classes of labels. We used 80% of the data as the training dataset and the others as the validation dataset. From Fig. 7, it is clear that our proposed AoA estimator achieved an accuracy of 97.67% in AoA classification.

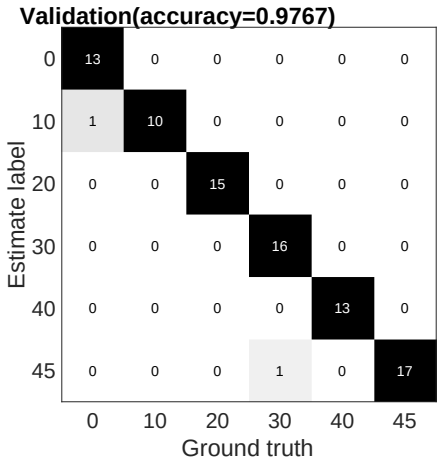

Fig. 7 Confusion matrix of AoA classification task

4.2.2 Regression Performance

In this experiment, we used dataset 2 described previously and evaluated the performance of our approach in regression estimation. We also adjusted the distance between the receiver (i.e., our array of devices) and the transmitter (the mobile device). We aimed to demonstrate that our AoA estimation is not strictly dependent on distance and can achieve good performance across different distances.

From Table 1, the experiment showed that our method achieved 4.14 degrees of MAE when the distance was 1 meter and 4.37 degrees when the distance was 2 meters. Our method achieves similar performance across different distances, indicating that our AoA estimation approach can perform well regardless of the distance.

Moreover, to clearly show regression performance over the AoA ground-truth, we calculated the estimation errors at different angles. We visualized the estimation results, where the value at each angle in the figure represents the estimation MAE at that angle. Points closer to the origin indicate smaller MAE and better AoA estimation performance. According to Fig. 8, it is evident that AoA estimation near 90 degrees performed better, while estimates for angles near the range edges were less accurate. We hypothesized that this is due to the use of a regression-based prediction model, where data influencing the edge angles are less abundant compared to those near the center angles.

Table 1 Comparison between different distance between transmitter and receiver

Distance (m)	Mean Absolute Error (deg) ↓
1	4.14
2	4.37

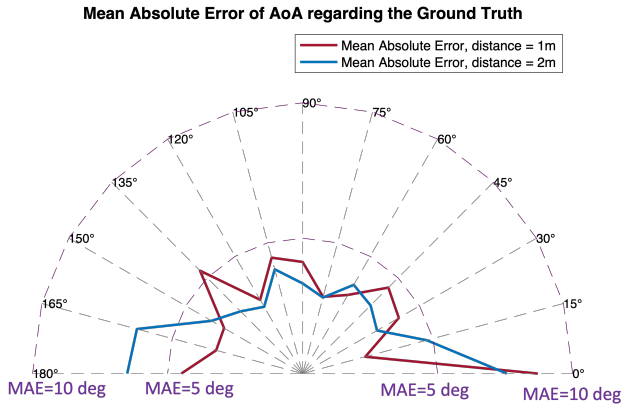

Fig. 8 MAE regarding different distance between transmitter and receiver

4.3 Results on different number of SISO devices and spacing

4.3.1 Comparison of different number of SISO devices

In this experiment, we demonstrated that forming an array with multiple SISO devices achieved better AoA prediction performance, thereby validating the effectiveness of our approach.

To ensure a fair comparison, we varied only the number of devices while keeping the distance between the receiver and transmitter unchanged, maintaining the same experimental setup, data volume, and the spacings between devices.

From the experiment results in Table 2, we achieved 6.84 degrees of MAE when using only 1 SISO device, 5.22 degrees when using 2 of them, and 4.14 degrees when 3 SISO devices were aligned into an array, as we proposed. We visualized the result in Fig. 9. It is evident that under the same setup, more devices in the array resulted in better AoA prediction performance. This demonstrates that our proposed array of single-antenna devices can effectively enhance the performance of AoA estimation using CSI amplitude.

Table 2 Comparison between different number of devices

Device setting	Mean Absolute Error (deg) ↓
1-Raspberry Pi	6.84
2-Raspberry Pi	5.22
3-Raspberry Pi	4.14

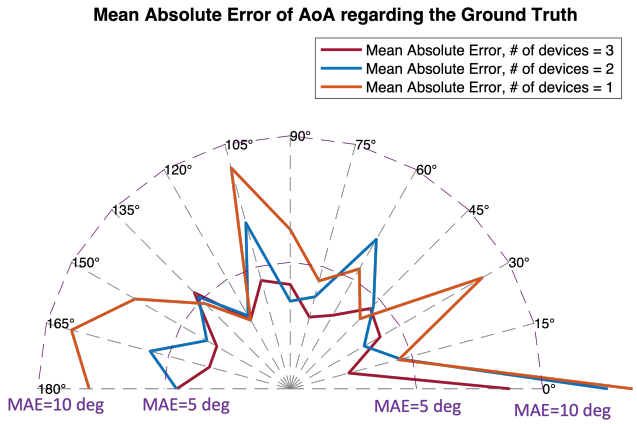

Fig. 9 MAE regarding different number of devices

4.3.2 Comparison of different spacing between devices

In this experiment, we used different spacing between each receiving device and evaluated the performance in AoA estimation. Generally, for AoA estimation methods based on CSI phase, adjusting the antenna spacing can help achieve better phase differences, with a commonly recommended spacing of half the wavelength. For 5GHz wireless signals, this distance is approximately 3cm. We aimed to verify whether this assumption still holds true for our amplitude-based approach.

We attempted to shorten the device spacing to 2cm, which is almost the shortest distance we could consider due to the thickness of the Raspberry Pi boards. However, the result in Table 3 shows that the MAE of 2cm spacing setting is only 6.51 degrees, which is worse than the result of the 4cm setting. As shown in Fig. 10, we observed that compared to a 4cm spacing, the new setup resulted in weaker estimation performance almost in all the ground-truth AoA labels. This might be due to the short spacing causing onboard antennas to be obstructed by other Raspberry Pi boards, leading to unwanted reflections, or because shorter distances are less conducive to extracting spatial information from amplitude. In fact, when using only amplitude, the phase information carried in the complex values of CSI is ignored, rendering the previous assumptions about device spacing inapplicable.

As part of future research, we will attempt to acquire more effective phase information or conduct experiments using external antennas. At that time, we will further explore and discuss the impact of device spacing.

Table 3 Comparison between different device spacing

Device spacing (cm)	Mean Absolute Error (deg) ↓
4	4.14
2	6.51

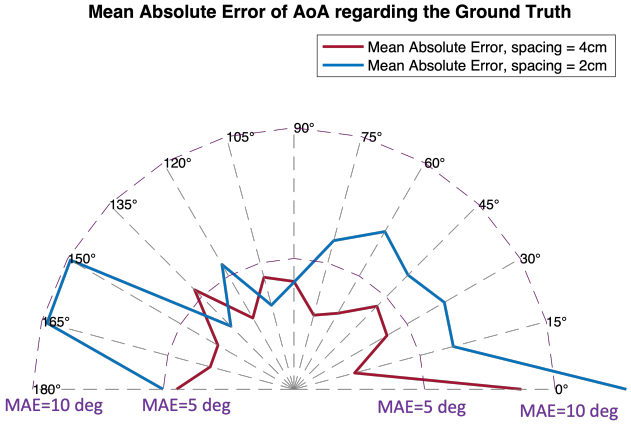

Fig. 10 MAE regarding different spacing between receiving devices

4.4 Discussion

AoA-based localization offers efficiency by focusing on physical information, but learning-based methods like ours and other CSI amplitude-based approaches, face cross-domain challenges requiring retraining in new environments, which we aim to address by correcting phase errors.

Generally, AoA obtained using WiFi is often used for indoor positioning. Compared to traditional techniques based on RSSI

or CSI fingerprinting, AoA-based localization focuses on obtaining physical information rather than more abstract signal features. This approach eliminates the need to collect fingerprint data at every location, thereby improving the efficiency of data collection for localization systems. Notably, using the 2D-MUSIC algorithm to classify signals does not require additional training data.

Since our method relies on learning-based AoA estimation, we must collect data across multiple angles, which increases the complexity of its application. At the same time, we did not address the cross-domain issue of the same model, which could result in a trained model being applicable to only one specific environment, making it less suitable for building a robust system.

It is worth noting that other proposed methods based on CSI amplitude also face the same issue, requiring retraining in different environments. We believe this problem is not unique to our proposal but rather caused by the inherent complexity of CSI signals. In the future, we will focus on how to correct phase errors in devices or explore ways to adapt a pre-trained model to different environments.

5. Conclusion

This study proposed a novel method utilizing an array of single-board Single Input Single Output (SISO) devices to extract Channel State Information (CSI) amplitude information for Angle of Arrival (AoA) prediction. This approach addresses the limitations of previous AoA estimation studies that relied on traditional MIMO capable devices, which are challenging to obtain in the market and difficult to scale. A frame header-based matching technique is proposed to align CSI data from the same frame received by different devices and adopted a learning-based approach to use the combined CSI from multiple devices as input to achieve AoA estimation results.

Multiple experiments demonstrated that our method achieved good AoA estimation performance with 4.14 degrees error in the optimal setting. We also tested various device configurations, including the impact of different numbers of devices, device spacing, and the distance between the receiver and transmitter. In the future, it is expected that this method can serve as a foundational implementation for studies aiming to extract AoA information from wireless data packets, offering not only easily accessible devices but also reliable estimation performance.

References

[1] Mariakakis, A. T., Sen, S., Lee, J. and Kim, K.-H.: SAIL: single access point-based indoor localization, *Proceedings of the 12th Annual International Conference on Mobile Systems, Applications, and Services*, MobiSys '14, Association for Computing Machinery, p. 315–328 (2014).

[2] Wu, K., Xiao, J., Yi, Y., Chen, D., Luo, X. and Ni, L. M.: CSI-Based Indoor Localization, *IEEE Transactions on Parallel and Distributed Systems*, Vol. 24, No. 7, pp. 1300–1309 (2013).

[3] Gao, Z., Gao, Y., Wang, S., Li, D. and Xu, Y.: CRISLoc: Reconstructable CSI Fingerprinting for Indoor Smartphone Localization, *IEEE Internet of Things Journal*, Vol. 8, No. 5, pp. 3422–3437 (2021).

[4] Ding, J. and Wang, Y.: WiFi CSI-Based Human Activity Recognition Using Deep Recurrent Neural Network, *IEEE Access*, Vol. 7, pp. 174257–174269 (2019).

[5] Schäfer, J., Barrsiwal, B. R., Kokhkharova, M., Adil, H. and Liebehenschel, J.: Human Activity Recognition Using CSI Information with Nexmon, *Applied Sciences*, Vol. 11, No. 19 (2021).

[6] Wang, X., Gao, L., Mao, S. and Pandey, S.: CSI-Based Fingerprinting for Indoor Localization: A Deep Learning Approach, *IEEE Transactions on Vehicular Technology*, Vol. 66, No. 1, pp. 763–776 (2017).

[7] Kotaru, M., Joshi, K., Bharadia, D. and Katti, S.: SpotFi: Decimeter Level Localization Using WiFi, *Proceedings of the 2015 ACM Conference on Special Interest Group on Data Communication*, SIGCOMM '15, Association for Computing Machinery, p. 269–282 (2015).

[8] Ma, Y., Zhou, G. and Wang, S.: WiFi Sensing with Channel State Information: A Survey, *ACM Comput. Surv.*, Vol. 52, No. 3 (2019).

[9] Zheng, Y., Sheng, M., Liu, J. and Li, J.: Exploiting AoA Estimation Accuracy for Indoor Localization: A Weighted AoA-Based Approach, *IEEE Wireless Communications Letters*, Vol. 8, No. 1, pp. 65–68 (2019).

[10] Ge, Y., Wang, J., Li, S., Qi, L., Zhu, S., Cooper, J., Imran, M. and Abbasi, Q. H.: WiFi sensing of Human Activity Recognition using Continuous AoA-ToF Maps, *2023 IEEE Wireless Communications and Networking Conference (WCNC)*, pp. 1–6 (2023).

[11] Fukushima, T., Murakami, T., Abeysekera, H., Fujihashi, T., Watanabe, T. and Saruwatari, S.: Feasibility Study of Practical AoA Estimation Using Compressed CSI on Commercial WLAN Devices, *IEEE Access*, Vol. 10, pp. 49128–49141 (2022).

[12] Kumrai, T., Cai, Z., Maekawa, T., Hara, T., Ohara, K., Murakami, T. and Abeysekera, H.: AoA-net: Estimating Angle-of-arrival Using Wi-Fi Channel State Information Based on Deep Neural Networks with Subcarrier Selection, *Journal of Information Processing*, Vol. 32, pp. 863–872 (2024).

[13] Halperin, D., Hu, W., Sheth, A. and Wetherall, D.: Tool Release: Gathering 802.11n Traces with Channel State Information, *ACM SIGCOMM CCR*, Vol. 41, No. 1, p. 53 (2011).

[14] Yan, K., Wang, F., Qian, B., Ding, H., Han, J. and Wei, X.: Person-in-WiFi 3D: End-to-End Multi-Person 3D Pose Estimation with Wi-Fi, *Proceedings of the IEEE/CVF Conference on Computer Vision and Pattern Recognition (CVPR)*, pp. 969–978 (2024).

[15] Hu, F., Cai, Y., Zhu, H., Chang, S., Wang, X. and Guo, M.: DeepAoA+: Online Cross-Domain Vehicular Relative Direction Estimation via Deep Learning, *IEEE Transactions on Vehicular Technology*, Vol. 73, No. 12, pp. 19216–19228 (2024).

[16] Gringoli, F., Schulz, M., Link, J. and Hollick, M.: Free Your CSI: A Channel State Information Extraction Platform For Modern Wi-Fi Chipsets, *Proceedings of the 13th International Workshop on Wireless Network Testbeds, Experimental Evaluation & Characterization*, WiNTECH '19, Association for Computing Machinery, p. 21–28 (2019).